

44. T. Nakajima *et al.*, *Cell* **90**, 1107 (1997).
 45. R. P. Kwok *et al.*, *Nature* **370**, 223 (1994).
 46. Y. Cui *et al.*, *Cell* **135**, 549 (2008).
 47. S. Ruediger *et al.*, *Nature* **473**, 514 (2011).

Acknowledgments: We thank C. M. Fletcher, A. Heynen, C. Alberini, C. Jennings, R. Desimone, M. Baratta, J. Biedenapp, R. Froemke, J. Czerniawski, and D. Bambah-Mukku for critical reading of the manuscript. We also thank G. Hale and M. Wilson for help characterizing the *Npas4^{-/-}* mice

and S. Ramirez for help with the open field assay. Y.L. acknowledges the generous support of the McGovern Institute for Brain Research at MIT. This work was supported by the MIT Presidential Marcus Fellowship to Honor Norman B. Leventhal (K.R.), a postdoctoral fellowship from the MIT Simons Initiative on Autism and the Brain (G.M.B), NSF grant IOS 0919159 (T.O.), a Whitehall Foundation research grant, an Anonymous Foundation research grant, the John Merck Scholar Program, and NIH grant MH091220-01 (Y.L.).

Supporting Online Material

www.sciencemag.org/cgi/content/full/334/6063/1669/DC1
 Materials and Methods
 SOM Text
 Figs. S1 to S7
 References (48–53)

9 May 2011; accepted 21 October 2011
 10.1126/science.1208049

How a DNA Polymerase Clamp Loader Opens a Sliding Clamp

Brian A. Kelch,^{1*} Debora L. Makino,^{1*†} Mike O'Donnell,² John Kuriyan^{1,3,4,5‡}

Processive chromosomal replication relies on sliding DNA clamps, which are loaded onto DNA by pentameric clamp loader complexes belonging to the AAA+ family of adenosine triphosphatases (ATPases). We present structures for the ATP-bound state of the clamp loader complex from bacteriophage T4, bound to an open clamp and primer-template DNA. The clamp loader traps a spiral conformation of the open clamp so that both the loader and the clamp match the helical symmetry of DNA. One structure reveals that ATP has been hydrolyzed in one subunit and suggests that clamp closure and ejection of the loader involves disruption of the ATP-dependent match in symmetry. The structures explain how synergy among the loader, the clamp, and DNA can trigger ATP hydrolysis and release of the closed clamp on DNA.

Chromosomal DNA replication relies on multiprotein replicases that copy DNA with high speed and processivity (1, 2). The polymerase subunits of the replicase are tethered to ring-shaped sliding clamps that encircle DNA, allowing the polymerase to bind and release DNA repeatedly without dissociating from the progressing replication fork. All replicases use a conserved sliding clamp mechanism for processivity (3–6), even though the bacterial and eukaryotic replicative polymerases have evolved independently (7, 8). Sliding clamps are also used for scanning DNA in several DNA repair processes (9).

Sliding clamps cannot load onto DNA spontaneously because they are closed circles (5, 10, 11) (Fig. 1A). Instead, adenosine triphosphate (ATP)-dependent complexes known as clamp loaders open the sliding clamps and load them onto primed DNA in the correct orientation for productive engagement of the polymerase [the clamp loaders are the γ/τ complex in bacteria, replication factor-C (RFC) in eukaryotes and archaea, and

¹Department of Molecular and Cell Biology and California Institute for Quantitative Biosciences, University of California, Berkeley, CA 94720, USA. ²Howard Hughes Medical Institute, Rockefeller University, New York, NY 10021, USA. ³Department of Chemistry, University of California, Berkeley, CA 94720, USA. ⁴Howard Hughes Medical Institute, University of California, Berkeley, CA 94720, USA. ⁵Physical Biosciences Division, Lawrence Berkeley National Laboratory, Berkeley, CA 94720, USA.

*These authors contributed equally to this work.

†Present address: Max Planck Institute of Biochemistry, Department of Structural Cell Biology, D-82152 Martinsried, Germany.

‡To whom correspondence should be addressed. E-mail: kuriyan@berkeley.edu

gp44/62 in T4 bacteriophage (Fig. 1B)]. Clamp loaders are members of the AAA+ superfamily of adenosine triphosphatases (ATPases), a diverse group of oligomeric ATPases whose functions

include motor and helicase activity and the ability to disassemble protein complexes (12, 13). In contrast to typical AAA+ ATPases, all clamp loader complexes are pentameric rather than hexameric. The lack of the sixth subunit in the clamp loader creates a gap in the assembly that is essential for the specific recognition of primer-template junctions (14, 15). The five subunits of the clamp loader are designated A, B, C, D, and E and are identified in Fig. 1B.

Each clamp loader subunit consists of three domains that are conserved in structure (14, 16–19). The first two of these domains form a AAA+ ATPase module, and five of these modules are brought together in intact clamp loaders such that ATP can be bound at interfacial sites (14) (Fig. 1B). The third conserved domain in each subunit is integrated into a circular collar that holds the assembly together in the absence of ATP.

A key role for ATP in the mechanism of clamp loaders is to trigger the formation of a spiral arrangement of AAA+ modules, leading to

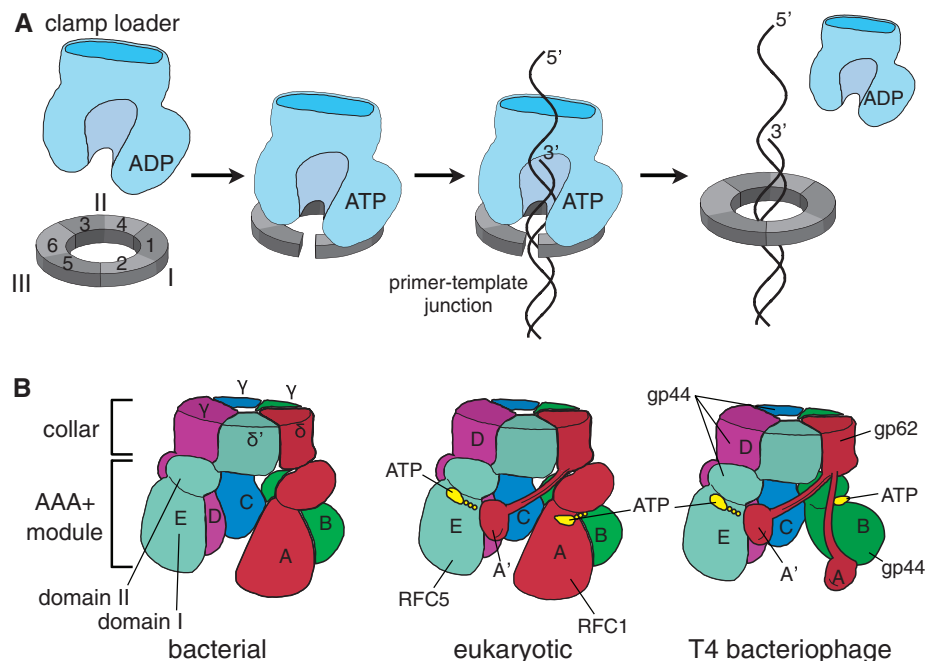


Fig. 1. Clamp loaders and sliding clamps. **(A)** Clamp-loading reaction. The clamp loader has low affinity for both clamp and primer-template DNA in the absence of ATP. Upon binding ATP, the clamp loader can bind the clamp and open it. The binding of primer-template DNA activates ATP hydrolysis, leading to ejection of the clamp loader. **(B)** Three classes of clamp loaders. Bacterial clamp loaders are pentamers consisting of three proteins: δ (A position), γ (B, C, and D positions), and δ' (E position). Eukaryotic clamp loaders (RFCs) consist of five different proteins, with the A subunit containing an A' domain that bridges the gap between the A and E AAA+ modules. The T4 bacteriophage clamp loader consists of two proteins: gp44 (the B, C, D, and E subunits) and gp62 (the A subunit).

the recognition of duplex DNA within the interior of the spiral (14–16). Biochemical data demonstrate that ATP binding also enables the clamp loader to bind to and open the sliding clamp (20) and that the binding of DNA triggers ATP hydrolysis and release of the closed clamp on DNA (21, 22). A molecular understanding of the mechanism that integrates clamp opening with its loading onto DNA is lacking because none of the structures of clamp loaders that have been determined so far include all four components of the active complex: the clamp loader, ATP, primer-template DNA, and the clamp. We now report structures of a clamp loader complex from bacteriophage T4 in which all of these components are present.

Organization of the T4 clamp loader complex.

We crystallized the T4 bacteriophage clamp loader bound to an ATP analog, primer-template DNA and the sliding clamp. The T4 replicase has served as a key model system in studies of DNA replication (1, 23), but the T4 clamp loader had not been characterized structurally. We determined structures from three distinct crystal forms, to resolutions of 3.5 Å (form I), 3.3 Å (form II), and 3.2 Å (form III), respectively (table S1). The T4 clamp consists of three copies of the gp45 protein (24). The general organization of the T4 clamp loader is similar to that of its bacterial and eukaryotic counterparts; it consists of one copy of the gp62 protein, located at the A position, and four copies of the gp44 protein (24), located at the B, C, D, and E positions (Fig. 2A).

The structure of gp44 is similar to that of a canonical clamp loader subunit, with a fully configured ATP binding site. The A subunit of the T4 clamp loader, gp62, is smaller than a canonical subunit (21 kD, versus 36 kD for gp44) because it lacks a AAA+ module, but the structure indicates that it is a minimal version of its eukaryotic homolog (Fig. 2A) (supporting online text). The A subunit has a collar domain, with a C-terminal extension, referred to as the A' domain, that has the same fold topology as the corresponding domain in the RFC-A subunit (14) (fig. S1). The A' domain bridges the gap between the A and E subunits to interact with the ATPase site of the E subunit, as seen in RFC (14). The structure of the T4 clamp loader complex resembles the general shape of a low-resolution electron microscopic reconstruction of an archaeal RFC bound to DNA and an open clamp (25) (fig. S2). Finally, although the AAA+ module has been replaced by a pair of helices in gp62, a flexible tether extending from these helices docks onto the clamp at the same site at which the RFC-A subunit docks onto PCNA (14).

The clamp loader holds the clamp in an open conformation. We trapped clamp loaders bound to open clamps in crystal forms I and II. There are two complexes in the asymmetric unit in crystal form I, and the clamp is open in one of these complexes and closed in the other. Crystal form II has one complex in the asymmetric unit, with the clamp open. The structures of the two

complexes with open clamps are similar, but the interactions between the clamp loader and the clamp are tighter in crystal form II, on which we focus our analysis. The two crystal forms were obtained with the same DNA construct, corresponding to a primer-template junction with a

20–base pair (bp) double-stranded segment and a 10-nucleotide single-stranded region. Ten base pairs of the double helix are within the interior of the clamp loader, and 10 bp are within the sliding clamp. The clamp loader and DNA have similar conformations in both com-

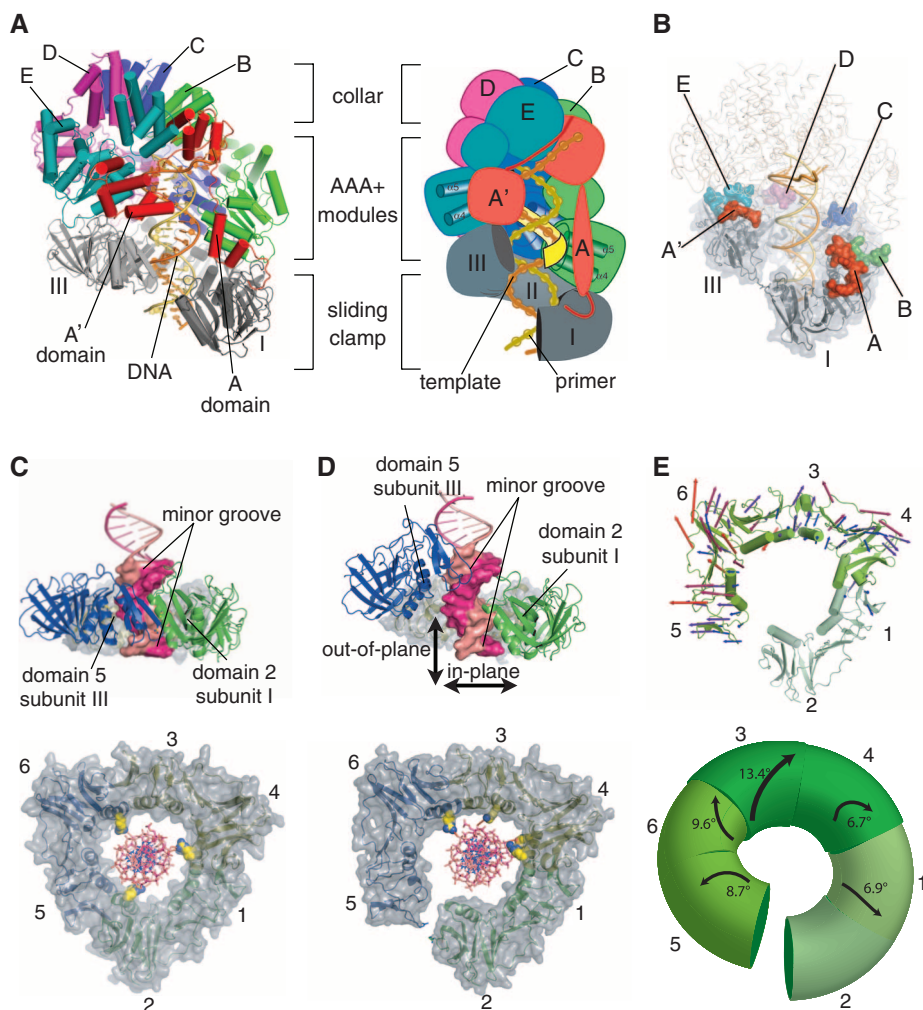


Fig. 2. Architecture of the T4 clamp loader–clamp–DNA complex (A) Structure of the T4 clamp loader bound to an open clamp. Ribbon and schematic diagrams of the complex between the T4 clamp loader (multicolored), the open T4 clamp (gray), which is broken between subunits I and III, and primer-template DNA. The gp62 protein (the A subunit; red) bridges the gap in the clamp with its A domain (a vestigial AAA+ module) on the lower part of the clamp and its A' domain at the top. The duplex region of primer-template DNA (orange) is bound in the interior of the clamp loader (yellow ribbon in the schematic indicates contacts from the clamp loader) and the central pore of the open clamp, with the template overhang extruded through the gap between the A and A' domains. (B) Interactions of the T4 clamp loader with the clamp. The six clamp interaction motifs of the clamp loader are displayed as surfaces with the remainder of the clamp loader shown as a thin ribbon. (C) Two orthogonal views of a closed clamp bound to DNA and the T4 clamp loader as in crystal form I. The clamp interacts with the DNA phosphate backbone through arginine residues from each clamp subunit (yellow). (D) Two orthogonal views of an open clamp bound to DNA and the T4 clamp loader. Diagram based on the open clamp complex in form II crystals. The side chains of Arg¹⁶² of subunit I and Arg⁸⁷ of subunit III are represented as sticks without the surface displayed. (E) Two representations of distortions in the structure of the open clamp, relative to that of the closed clamp. Top: Displacement vectors between the two structures are shown, scaled up by a factor of 4. The magnitude of the displacement is also indicated by color (blue to red). Vectors are drawn in the direction of displacement from the planar to open conformation and are derived from local alignments of each of the six pseudo-symmetric domains in the clamp trimer. Bottom: Domain rotations derived from these local alignments are mapped onto a schematic diagram of the open clamp.

plexes of crystal form I, but crystal lattice contacts result in partial disengagement of the clamp loader from the clamp in the complex with a closed clamp.

The opening of the clamp involves a switch from the closed planar ring-like structure (6) to an open right-handed lock washer shape. Extensive interactions between the surface of the sliding clamp and the undersurface of the clamp loader (the region distal to the collar domains) buries a total of $\sim 7200 \text{ \AA}^2$ of surface area and holds the clamp open (Fig. 2B). The clamp has three subunits (I, II, and III, defined in Fig. 1A), with each subunit consisting of two domains with similar structure (3, 6). The N- and C-terminal domains of subunits I, II, and III are numbered 1 and 2, 3 and 4, and 5 and 6, respectively (Fig. 1A). These are arranged in head-to-tail fashion in the order 2-1-4-3-6-5, with domains 2 and 1 interacting with subunits A and B, respectively, of the clamp loader, and ending with domain 5 interacting with the A' domain. The opening is due to breakage of the interface between domain 2 (beneath the A position of the clamp loader) and domain 5 (beneath the E subunit and the A' domain).

How the clamp opens can be appreciated by using the double-helical DNA within the clamp as a reference. In the complex with the closed clamp, the clamp loader positions the DNA so that its helical axis is aligned with the central axis of rotational symmetry of the clamp (Fig. 2C). The closed clamp makes limited contact with the DNA, mainly through ion-pairing interactions between arginine side chains in the central pore of the clamp and phosphate groups of DNA. This centered alignment of DNA within the closed clamp is distinct from the tipped orientation seen in crystal structures of DNA and clamps in isolation (26, 27).

The open clamp adopts a spiral that matches the helical geometry of DNA, with the helices

that line the inner surface of the clamp tracking the minor groove of DNA, but with limited contact. Each subunit of the clamp is related to the adjacent one by rotations about axes that are aligned with the helical axis of DNA. The lateral opening of the clamp results in the clamp domains nearest the opening (domains 2 and 5) moving away from the DNA (Fig. 2D).

Clamp opening results from the twisting of individual domains with respect to adjacent domains (Fig. 2E). The distortions are greatest at the region opposite the gap, with the largest overall change (a $\sim 13^\circ$ twist) between domains 3 and 4. Distortions at this site provide the greatest leverage for clamp opening.

Our structures allow us to address the mechanism by which primer-template DNA enters the central chamber of the open clamp-clamp loader complex. The opening of the clamp arises from an in-plane movement of $\sim 9 \text{ \AA}$ and an out-of-plane movement of $\sim 23 \text{ \AA}$. The resulting $\sim 9 \text{ \AA}$ gap between domains 2 and 5 in the open clamp is not wide enough to allow an extended double-helical segment to pass through (Fig. 2D). The extent of clamp opening seen in the crystal structure is likely to be close to that of the clamp-clamp loader complex prior to DNA binding because of extensive interactions between each of the five clamp loader subunits and the clamp, with the bound ATP stabilizing this conformation (see below). This is consistent with Förster resonance energy transfer (FRET) measurements of the extent of opening in the yeast clamp, which suggest that the gap in the open clamp-clamp loader complex constricts by only $\sim 1 \text{ \AA}$ upon DNA binding (28). The clamp loader has a small gap between the A and A' domains, which also narrows the portal into the interior chamber of the clamp loader.

Single-stranded DNA can pass through the gap between domains 2 and 5, with the primer-template duplex sliding into the interior chamber

of the clamp loader through the central pore of the sliding clamp. It is also possible that the single-stranded double-helix junction is recognized directly by the complex. The flexibility of the single-stranded portion might allow domain 5 in the open clamp to fit into the major groove of the double helix (fig. S3).

The clamp loader has six major points of contact with the open clamp: one each involving the B, C, D, and E subunits (gp44), and two separate interactions made by the A subunit (gp62) (Fig. 2B and fig. S5). Three of these contacts involve the canonical mechanism used by diverse proteins to engage sliding clamps, in which the docking sites on the clamp are each located within a single subunit, at the interface between the two domains that comprise the subunit (the A, C, and E subunits of the clamp loader dock in this way). The other three docking sites in the clamp are structurally analogous to the first three, but are located at the interfaces between different clamp subunits rather than within a single subunit. The B and D subunits of the clamp loader dock onto the two closed subunit interfaces of the clamp, while the A' domain docks onto the edge of subunit III, next to the broken interface in the clamp. In this way, all of the binding sites on the clamp are satisfied by the clamp loader (Fig. 2B).

Bacterial clamp loaders do not have a domain corresponding to the A' domain of the T4 and RFC clamp loaders. This difference may reflect the decreased stability of the trimeric PCNA and T4 clamps relative to the dimeric bacterial clamps (29). The bridging interaction made by the T4 and RFC clamp loaders may be necessary to prevent dissociation of subunit III when the trimeric clamps are opened.

A-form DNA is recognized by the clamp loader spiral. The interaction between the primer-template junction and the clamp loader is very similar to that defined earlier for the *Escherichia*

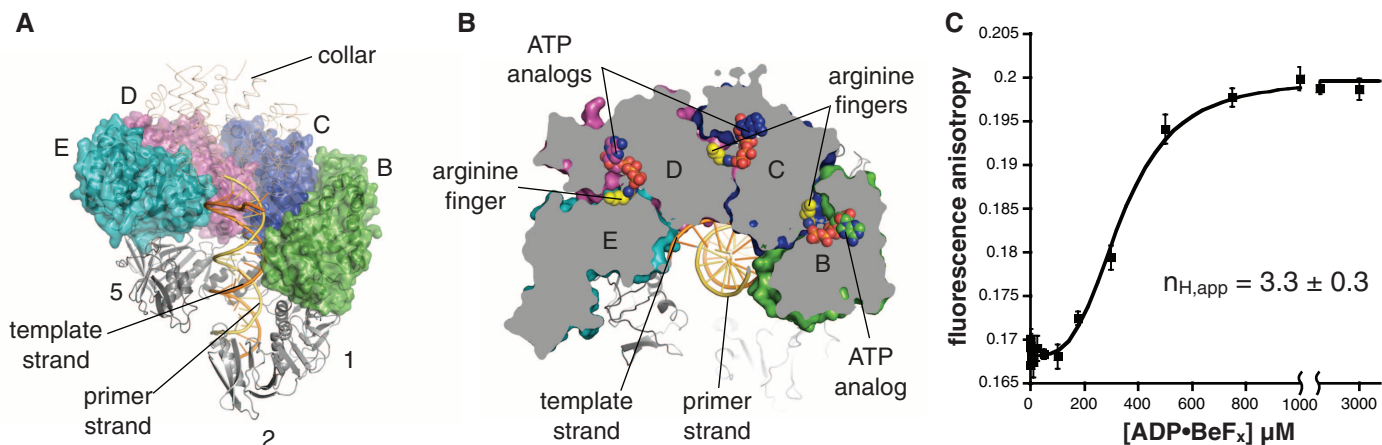


Fig. 3. Symmetric and cooperative recognition of DNA. **(A)** Spiral of AAA+ modules in the T4 clamp loader bound to an open clamp. The gp44 AAA+ modules, for which surfaces are displayed, form a spiral that tracks the minor groove of the DNA. The A subunit (gp62) is not shown. **(B)** Arginine fingers and ATP coordinate the AAA+ spiral and DNA binding. A top-down view with the arginine fingers and the ATP analog (ADP·BeF₃) shown as spheres (collar

domains not shown). **(C)** Cooperativity in ATP binding. The T4 clamp loader and the clamp, at concentrations of 2 and 5 μM , respectively, were incubated in the presence of 100 nM 5'TAMRA-labeled primer-template DNA. ADP·BeF_x was titrated into the solution. As the concentration of the ATP analog increases, DNA binds to the clamp loader and the fluorescence anisotropy of the TAMRA probe increases in a highly sigmoidal fashion ($n_{H,\text{app}} = 3.3 \pm 0.3$).

coli clamp loader (15). The duplex region lies within the inner chamber of the clamp loader, which orients it to thread through the central pore of the clamp. The closest contacts between clamp loader and DNA duplex are with the template strand (Fig. 3A and fig. S6A), thus accommodating both RNA and DNA primers. Primer-template junctions have the 3' end of the primer strand located at the double strand–single strand junction. Specificity for this DNA structure arises from blockage of the 3' end of the primer strand by the B subunit collar, and the binding of the template strand to an exit channel located in the gap between the A and A' domains (fig. S6B).

The clamp loader induces the template strand within the central chamber to switch from B-form to nearly A-form, resulting in a widening of the minor groove to accommodate loops from the AAA+ modules (fig. S6, C and D). Although the resolution of our analysis precludes unambiguous definition of the sugar conformation, the positioning of the 3' and 5' phosphate groups with respect to the sugar is consistent with the C3'-endo sugar pucker associated with A-form DNA or RNA. The DNA conformation is consistent with the natural RNA-DNA substrates of the clamp loader, which are known to be A-form (30).

The AAA+ modules form a symmetric spiral. As in other AAA+ ATPases, the key to clamp loader function is the interfacial coordination of ATP bound to one subunit by residues presented by an adjacent subunit, most prominently an invariant “arginine finger” (31, 32). Adenosine diphosphate (ADP)–BeF₃ ligands can be identified clearly at the B, C, and D subunits of the T4 clamp loader (fig. S7), with interfacial coordination of the BeF₃ moiety, corresponding to the γ -phosphate of ATP, by the conserved arginine finger side chains (Arg¹⁵¹ in gp44; Fig. 3B). The A' domain does not present an arginine finger to the nucleotide bound to the E subunit. We therefore define the fully ATP-loaded form of the T4 clamp loader to have ATP in the B, C, and D subunits, with either ADP or ATP in the E subunit.

In the ATP-bound state, the clamp binding motifs from the four AAA+ modules and the A subunit are arranged such that they match the periodicity of docking sites in the clamp (Fig. 2B and 3B). This is because the binding of DNA by the clamp loader induces a symmetric spiral arrangement of the AAA+ modules that matches the helicity of DNA (Fig. 3A) (15). In the T4 clamp loader, each AAA+ module rotates about the helical axis of the primer-template DNA by $\sim 60^\circ$, with a helical rise of ~ 8 Å, and binds 2.5 bp of DNA (1 bp is shared with an adjacent AAA+ module) (fig. S6A). Thus, the double helix templates the symmetric arrangement of the AAA+ modules, which then form a spiral platform for positioning the open clamp.

The symmetric and ATP-bridged conformations of AAA+ modules and their interactions

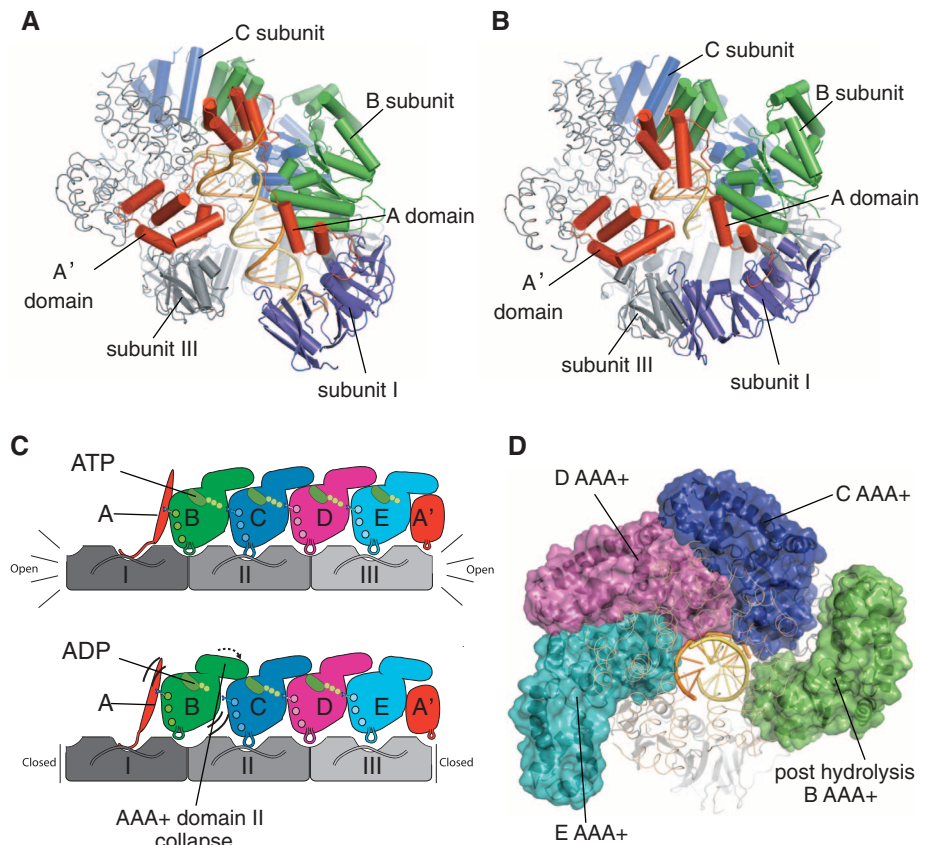


Fig. 4. Hydrolysis-induced conformational changes. **(A)** The fully ATP-bound conformation of the open clamp–clamp loader–DNA complex from form II crystals. The clamp loader holds the clamp such that there is a gap between subunits I and III of the clamp. **(B)** Conformational changes in the clamp–clamp loader–DNA complex from ATP hydrolysis at the B subunit as seen in form III crystals. The structure of the complex is shown in the same orientation as in Fig. 4A (superposed using the AAA+ module of the C subunit). Clamp subunits I and III are sealed so that the clamp is now closed. The A and B subunits, as well as the entire collar region, undergo a large conformational change. **(C)** Schematic diagram describing ATP hydrolysis-induced changes in clamp interactions. The clamp and the AAA+ modules of the clamp loader are shown from the side. In the ATP-loaded state, all AAA+ modules are positioned perfectly to match the clamp binding sites. Upon ATP hydrolysis, the B subunit swings away from the C subunit, altering the spacing between the clamp binding loops. **(D)** ATP hydrolysis severs contacts between AAA+ modules. The AAA+ modules are shown as surfaces. The interface between the B and C AAA+ modules has been completely disrupted.

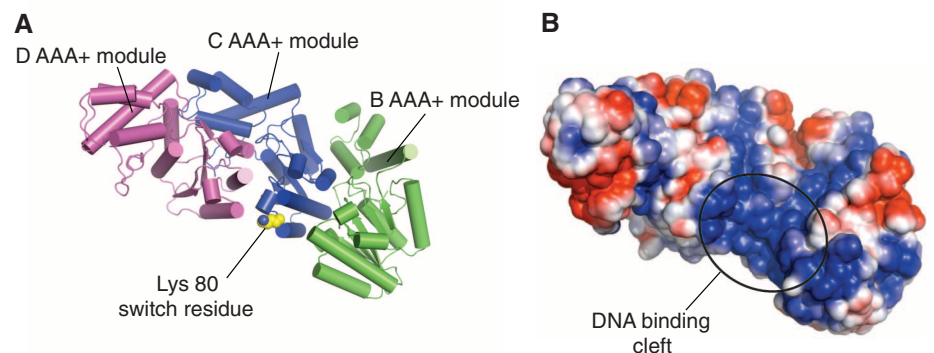


Fig. 5. A proposed DNA-dependent allosteric switch. **(A)** The switch residue of the T4 clamp loader (Lys⁸⁰) is pointing into the interior chamber of the clamp loader to interact with DNA (DNA not shown). **(B)** In the absence of DNA, the calculated electrostatic potential is extremely positive in the DNA binding cleft (calculation performed without Mg²⁺ or ADP–BeF₃ ligands).

with DNA suggest that the binding and hydrolysis of ATP will be cooperative in the presence of DNA. Conversely, the AAA+ modules of the clamp loader might also disengage from each other cooperatively upon ATP hydrolysis, promoting the dissociation of the clamp loader from DNA despite its interactions with DNA and the clamp.

Indeed, we show that binding of the ATP analog ADP-BeF_x to the T4 clamp loader is cooperative in the presence of DNA (Fig. 3C and supporting online text). Additionally, the rate of ATP hydrolysis by the T4 clamp and clamp loader is cooperative with respect to ATP concentration in the presence of primer-template DNA, but not in its absence (33). The lack of cooperativity in the absence of DNA is consistent with the structure, because of the obvious coupling between different ATP binding sites provided by the DNA. Therefore, primer-template DNA induces the cooperative assembly of the clamp-clamp loader complex, and conversely triggers its cooperative disassembly (see below).

Structural consequences of ATP hydrolysis at one site in the complex. We determined a structure of the T4 clamp loader and clamp bound to

DNA at 3.2 Å resolution from a third crystal form (form III) (table S1), which corresponds to a state in which the B subunit has hydrolyzed ATP. These crystals were formed with ADP-BeF_x as before, but with DNA containing a 10-bp duplex with a 10-nucleotide template overhang. The duplex region is bound exclusively within the clamp loader. The clamp is closed in this structure, with ADP-BeF₃ bound only to subunits C and D (compare Fig. 4A with Fig. 4B). Electron density at the nucleotide binding site in subunit B indicates that only ADP is bound at this site (fig. S9A).

The structure reveals a conformational change in the clamp loader in which the B subunit AAA+ module moves away from the C subunit by ~7 Å, toward the gap between the A and A' domains, thereby partially disengaging from the template strand and the clamp (Fig. 4, C and D). The N-terminal domain of the A subunit is tightly anchored to the B subunit through hydrophobic contacts and therefore these two domains do not change their relative position. The A subunit also remains docked to the clamp because of flexibility in the docking segment. The contacts made by the C, D, and E subunits to the clamp and to

each other in the AAA+ spiral are also largely maintained. Thus, the conformational change in B is correlated with closure of the clamp, consistent with studies indicating that a single ATP hydrolysis event is sufficient to close the clamp (34).

ATP hydrolysis in the B subunit alters the structure of the AAA+ module such that domain II collapses onto domain I, rotating ~15° about an axis running through the vacated site for the γ-phosphate of ATP. The new conformation of domain II in the B subunit is incompatible with the symmetric spiral of AAA+ modules because of steric clash with domain I of the C subunit (Fig. 4C). Comparison of the T4 clamp loader with other AAA+ ATPases (35, 36) shows that collapse of domain II in response to ATP hydrolysis is a conserved feature of this family (fig. S10).

We propose that hydrolysis of ATP initiates at the B site. This induces a conformational change in the clamp loader with minimal disruption of the contacts to the clamp and the DNA. The B subunit releases from the template strand upon ATP hydrolysis, and when the T4 clamp loader is bound to its natural target (a 5-bp RNA-DNA primer) the template strand interacting with the B subunit is single-stranded and is more likely to disengage because of flexibility. The movement of the B subunit provides room for the release of the C subunit from D. The ability of B to move away from C readily will also promote ATP hydrolysis at B by enabling release of the phosphate ion, which would otherwise be trapped within the buried interfacial sites. Initiation of hydrolysis at the B site is also suggested by comparison to F₁-ATPase, in which the opening of one nucleotide-binding site provides direction to the ATPase cycle (37, 38). As ATP hydrolysis continues up the AAA+ spiral, the symmetry matching of the clamp loader with the DNA and clamp is broken progressively, leading to dissociation of the clamp loader.

Stimulation of ATP hydrolysis by DNA. Clamp loader ATPase activity is stimulated by binding of primer-template DNA (21), but the mechanism of activation is unclear. We note a striking DNA-dependent rearrangement of a conserved DNA binding residue that affects the conformation of a catalytic glutamate in the conserved Walker B motif. In the absence of DNA, as seen in the yeast clamp-clamp loader structure (14), the backbone of the catalytic glutamate (Glu⁴²⁵ in yeast RFC-A) in the Walker B motif is held in an inactive conformation by a conserved basic residue (the “switch” residue; e.g., Arg³⁸³ in RFC-A; fig. S11A). Conversely, in the structure of the T4 clamp loader bound to DNA, the switch residue (Lys⁵⁰ in gp44) is not in the interior of the protein, but instead interacts directly with the phosphate backbone of the template strand (fig. S11B). This releases the carbonyls of the Walker B motif to adopt an alternate hydrogen-bonding pattern and the glutamate acquires an active conformation.

We propose that electrostatic repulsion generated by positively charged residues and helix

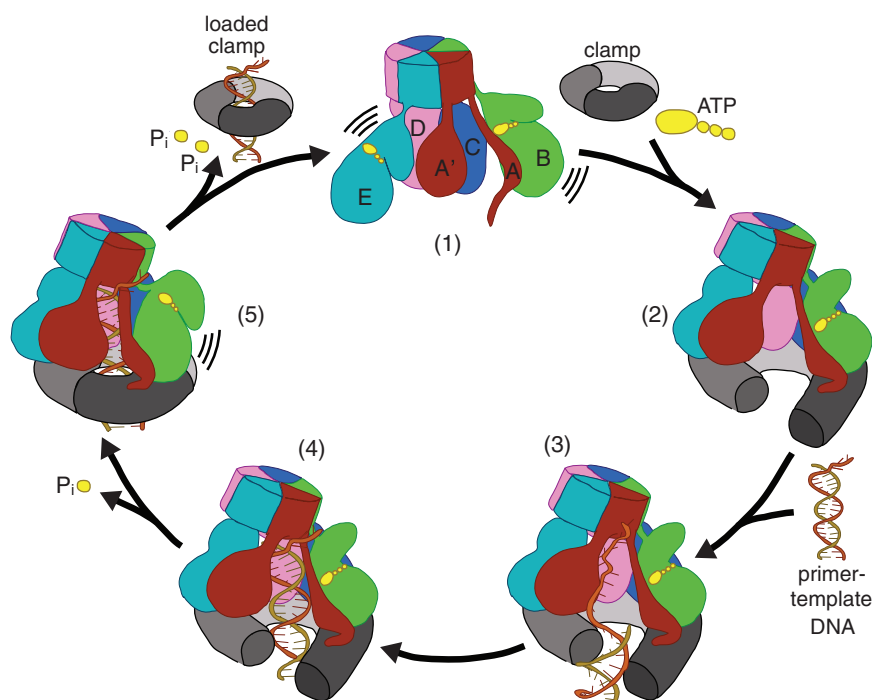


Fig. 6. A detailed mechanism for the clamp loading reaction. The reaction cycle for the T4 clamp loader is shown as a schematic diagram. (1) In the absence of ATP, the clamp loader AAA+ modules cannot organize into a spiral shape. (2) Upon ATP binding, the AAA+ modules form a spiral that can bind and open the clamp. (3) Primer-template DNA must thread through the gaps between the clamp subunits I and III and the clamp loader A and A' domains. (4) Upon DNA binding in the interior chamber of the clamp loader, ATP hydrolysis is activated, most likely through flipping of the switch residue and release of the Walker B glutamate. (5) ATP hydrolysis at the B subunit breaks the interface at the AAA+ modules of the B and C subunits and allows closure of the clamp around primer-template DNA. Further ATP hydrolyses at the C and D subunits dissolve the symmetric spiral of AAA+ modules, thus ejecting the clamp loader because the recognition of DNA and the clamp is broken. The clamp is now loaded onto primer-template DNA, and the clamp loader is free to recycle for another round of clamp loading.

dipoles at the DNA binding interface favors the inward movement of the switch residue in the absence of DNA (Fig. 5). The DNA-dependent flipping of the switch residue appears to be conserved, even in the more distantly related bacterial clamp loaders. In the structure of *E. coli* clamp loader bound to primer-template DNA, the switch residue in the B, C, and D subunits (Lys¹⁰⁰ in *E. coli* γ subunit) makes direct contact with the DNA phosphate backbone (fig. S11, C and D) (15). In the absence of DNA, this residue is buried in the interior of the AAA+ modules (16).

We suggest that DNA binding to the clamp loader has two effects that favor ATP hydrolysis: (i) stabilization of the symmetric AAA+ spiral and placement of the arginine fingers at the neighboring active sites (15), and (ii) flipping of the allosteric switch that couples DNA binding to the Walker B motif. Reexamination of mutational data for the *E. coli* clamp loader (39) provides experimental evidence for this allosteric switch. When the switch residue is mutated to glutamate, which is expected to favor the active conformation of the catalytic glutamate in the Walker B motif, the basal ATPase activity of the clamp loader increases by ~50%. Mutation of nearby Arg⁸⁸ to glutamate, which we also expect to flip out the switch residue via electrostatic attraction, increases the basal ATPase rate by nearly a factor of 2. Mutations farther from the switch residue do not change the basal ATPase rate.

Conclusions. Our analysis provides a detailed molecular mechanism for how clamp loaders couple ATP binding and release to the loading of sliding clamps onto DNA (Fig. 6). Clamp loaders use the helical symmetry of DNA to recognize primer-template junctions and to complete the formation of catalytically competent ATPase active sites. Thus, recognition of the DNA target by a clamp-clamp loader complex triggers the disassembly of the loader complex and the release of the closed clamp on DNA. As shown previously for the *E. coli* clamp loader complex bound to DNA (15), the AAA+ modules of the ATP-loaded clamp loader are organized symmetrically, so that they match the geometry of the double helix. Our structures of the T4 clamp loader now show that the sliding clamp also adopts an open spiral structure that matches the geometry of DNA, thereby allowing a stable interaction with the ATP-bound clamp loader.

The T4 sliding clamp is highly dynamic (40) and is likely to convert between open and closed forms spontaneously. The principal function of the T4 clamp loader is likely to trap the open form of the clamp and load it onto primer-template DNA in the correct orientation for productive coupling to the polymerase. In other systems, the clamp loader may also play an active role in opening the closed clamp. The bacterial clamps, for example, are very stable and likely to be closed unless opened actively. The A subunit (δ) of the bacterial clamp loader induces a con-

formational change in the sliding clamp that opens it (22, 41), which may be a required first step in the clamp loader process. Despite these differences in the nature of the initial encounter, the structural elements of the integrated interfaces between the AAA+ modules of the clamp loader and the DNA double helix are virtually superimposable between the *E. coli* and T4 structures. This structural conservation indicates that the clamp-loading mechanism has remained essentially unchanged since the dawn of the DNA world.

Our structures provide an unprecedented view of a AAA+ machine bound to two macromolecular substrates—the sliding clamp and DNA—thereby revealing how the binding and hydrolysis of ATP is coordinated by templating the structure of the protein assemblies on the DNA double helix. A common aspect to all AAA+ ATPases appears to be the generation of a helical displacement between adjacent subunits that have ATP bound between them. In the functional states of hexameric motor proteins and helicases, a symmetric helical arrangement of the AAA+ modules is interrupted because not all of the subunits in the assembly bind ATP simultaneously (42, 43). In the case of clamp loaders, the cooperative binding of ATP to all functional sites leads to coordinated ATP hydrolysis and disassembly of the complex from the macromolecular substrates, which is a key aspect to the function of clamp loaders as molecular matchmakers (44).

References and Notes

1. S. J. Benkovic, A. M. Valentine, F. Salinas, *Annu. Rev. Biochem.* **70**, 181 (2001).
2. R. T. Pomerantz, M. O'Donnell, *Trends Microbiol.* **15**, 156 (2007).
3. Y. Shamoto, T. A. Steitz, *Cell* **99**, 155 (1999).
4. T. S. Krishna, X. P. Kong, S. Gary, P. M. Burgers, J. Kuriyan, *Cell* **79**, 1233 (1994).
5. X. P. Kong, R. Onrust, M. O'Donnell, J. Kuriyan, *Cell* **69**, 425 (1992).
6. I. Moarefi, D. Jeruzalmi, J. Turner, M. O'Donnell, J. Kuriyan, *J. Mol. Biol.* **296**, 1215 (2000).
7. S. Bailey, R. A. Wing, T. A. Steitz, *Cell* **126**, 893 (2006).
8. M. H. Lamers, R. E. Georgescu, S.-G. Lee, M. O'Donnell, J. Kuriyan, *Cell* **126**, 881 (2006).
9. C. E. Helt, W. Wang, P. C. Keng, R. A. Bambara, *Cell Cycle* **4**, 529 (2005).
10. R. Onrust, P. T. Stukenberg, M. O'Donnell, *J. Biol. Chem.* **266**, 21681 (1991).
11. P. T. Stukenberg, P. S. Studwell-Vaughan, M. O'Donnell, *J. Biol. Chem.* **266**, 11328 (1991).
12. A. F. Neuwald, L. Aravind, J. L. Spouge, E. V. Koonin, *Genome Res.* **9**, 27 (1999).
13. J. P. Erzberger, J. M. Berger, *Annu. Rev. Biophys. Biomol. Struct.* **35**, 93 (2006).
14. G. D. Bowman, M. O'Donnell, J. Kuriyan, *Nature* **429**, 724 (2004).
15. K. R. Simonetta *et al.*, *Cell* **137**, 659 (2009).
16. D. Jeruzalmi, M. O'Donnell, J. Kuriyan, *Cell* **106**, 429 (2001).
17. T. Oyama, Y. Ishino, I. K. Cann, S. Ishino, K. Morikawa, *Mol. Cell* **8**, 455 (2001).
18. A. Seybert, M. R. Singleton, N. Cook, D. R. Hall, D. B. Wigley, *EMBO J.* **25**, 2209 (2006).
19. B. Guenther, R. Onrust, A. Sali, M. O'Donnell, J. Kuriyan, *Cell* **91**, 335 (1997).

20. M. M. Hingorani, M. O'Donnell, *J. Biol. Chem.* **273**, 24550 (1998).
21. T. C. Jarvis, L. S. Paul, J. W. Hockensmith, P. H. von Hippel, *J. Biol. Chem.* **264**, 12717 (1989).
22. J. Turner, M. M. Hingorani, Z. Kelman, M. O'Donnell, *EMBO J.* **18**, 771 (1999).
23. M. C. Young, M. K. Reddy, P. H. von Hippel, *Biochemistry* **31**, 8675 (1992).
24. T. C. Jarvis, L. S. Paul, P. H. von Hippel, *J. Biol. Chem.* **264**, 12709 (1989).
25. T. Miyata *et al.*, *Proc. Natl. Acad. Sci. U.S.A.* **102**, 13795 (2005).
26. R. E. Georgescu *et al.*, *Cell* **132**, 43 (2008).
27. R. McNally, G. D. Bowman, E. R. Goedken, M. O'Donnell, J. Kuriyan, *BMC Struct. Biol.* **10**, 3 (2010).
28. Z. Zhuang, B. L. Yoder, P. M. J. Burgers, S. J. Benkovic, *Proc. Natl. Acad. Sci. U.S.A.* **103**, 2546 (2006).
29. N. Yao *et al.*, *Genes Cells* **1**, 101 (1996).
30. O. Yu. Fedoroff, M. Salazar, B. R. Reid, *J. Mol. Biol.* **233**, 509 (1993).
31. A. Johnson, M. O'Donnell, *J. Biol. Chem.* **278**, 14406 (2003).
32. M. R. Ahmadian, P. Stege, K. Scheffzek, A. Wittinghofer, *Nat. Struct. Biol.* **4**, 686 (1997).
33. P. Pietroni, P. H. von Hippel, *J. Biol. Chem.* **283**, 28338 (2008).
34. P. Pietroni, M. C. Young, G. J. Latham, P. H. von Hippel, *J. Mol. Biol.* **309**, 869 (2001).
35. J. P. Erzberger, M. L. Mott, J. M. Berger, *Nat. Struct. Mol. Biol.* **13**, 676 (2006).
36. J. Wang *et al.*, *Structure* **9**, 1107 (2001).
37. Y. Q. Gao, W. Yang, M. Karplus, *Cell* **123**, 195 (2005).
38. J. P. Abrahams, A. G. Leslie, R. Lutter, J. E. Walker, *Nature* **370**, 621 (1994).
39. E. R. Goedken, S. L. Kazmirski, G. D. Bowman, M. O'Donnell, J. Kuriyan, *Nat. Struct. Mol. Biol.* **12**, 183 (2005).
40. S. C. Alley *et al.*, *Biochemistry* **38**, 7696 (1999).
41. D. Jeruzalmi *et al.*, *Cell* **106**, 417 (2001).
42. E. J. Enemark, L. Joshua-Tor, *Nature* **442**, 270 (2006).
43. S. E. Glynn, A. Martin, A. R. Nager, T. A. Baker, R. T. Sauer, *Cell* **139**, 744 (2009).
44. A. Sancar, J. E. Hearst, *Science* **259**, 1415 (1993).

Acknowledgments: We thank K. Morikawa for providing the molecular envelope from the electron microscopic reconstruction of the archaeal clamp loader complex, P. von Hippel, S. Tsutakawa, and S. Benkovic as well as Kuriyan lab members for helpful discussions. We thank K. Engel for creating Fig. 6, K. Simonetta for providing *E. coli* clamp loader protein for ADP-BeF_x titrations, and the staff at Beamlines 8.2.1, 8.2.2 and 8.3.1 of the Advanced Light Source, which is supported by U.S. Department of Energy under contract DE-AC03-76SF00098. This work was partially supported by NIH grants F32-087888 (B.K.), R01-GM308839 (M.O.D.), and R01-GM45547 (J.K.). The authors declare no conflict of interest. B.K., D.M. and J.K. designed experiments. B.K. and D.M. performed experiments. B.K., D.M., M.O.D., and J.K. analyzed the data. B.K. and J.K. wrote the paper. Coordinates and structure factors have been deposited in the Protein Data Bank with accession codes 3U5Z, 3U60, and 3U61 for crystal forms I, II, and III, respectively.

Supporting Online Material

www.sciencemag.org/cgi/content/full/334/6063/1675/DC1
Materials and Methods
Figs. S1 to S11
Tables S1 and S2
References (45–61)

29 July 2011; accepted 31 October 2011
10.1126/science.1211884

This copy is for your personal, non-commercial use only.

If you wish to distribute this article to others, you can order high-quality copies for your colleagues, clients, or customers by [clicking here](#).

Permission to republish or repurpose articles or portions of articles can be obtained by following the guidelines [here](#).

The following resources related to this article are available online at www.sciencemag.org (this information is current as of July 25, 2015):

Updated information and services, including high-resolution figures, can be found in the online version of this article at:

<http://www.sciencemag.org/content/334/6063/1675.full.html>

Supporting Online Material can be found at:

<http://www.sciencemag.org/content/suppl/2011/12/22/334.6063.1675.DC1.html>

A list of selected additional articles on the Science Web sites **related to this article** can be found at:

<http://www.sciencemag.org/content/334/6063/1675.full.html#related>

This article **cites 59 articles**, 17 of which can be accessed free:

<http://www.sciencemag.org/content/334/6063/1675.full.html#ref-list-1>

This article has been **cited by** 19 articles hosted by HighWire Press; see:

<http://www.sciencemag.org/content/334/6063/1675.full.html#related-urls>

This article appears in the following **subject collections**:

Biochemistry

<http://www.sciencemag.org/cgi/collection/biochem>